Experimental evidence for a continuous phase transition in a multidimensional ferroelectric

P. Czarnecki

Faculty of Physics, Adam Mickiewicz University, Umultowska 85, 60-614 Poznań, Poland

A. Katrusiak

Faculty of Chemistry, Adam Mickiewicz University, Grunwaldzka 6, 60-780 Poznań, Poland

I. Szafraniak and J. Wąsicki

Faculty of Physics, Adam Mickiewicz University, Umultowska 85, 61-614 Poznań, Poland
(Received 18 August 1997)

Two phase transitions in ferroelectric crystals of pyridinium tetrafluoroborate $[C_5H_6N]^+BF_4^-$ have been characterized by x-ray- and neutron-diffraction studies and measurements of permittivity, pyroeffect, and spontaneous polarization. At $T_1 = 238.7$ K the crystals transform from $R\bar{3}m$ to $C2$ symmetry, and at $T_2 = 204$ K to space group $P2$. The ions are orientationally disordered in the prototype phase, and the ferroelectricity below T_1 is induced by the onset of ordering of the ions. The spontaneous polarization of 1.5 μC/cm^2 was found from pyroelectric-effect measurements. The anisotropy measurements of permittivity indicate clearly that the phase transition at T_1 is continuous, which is the unique case corroborating Landau's approach of deducing the character of phase transitions from symmetry considerations for multidimensional ferroelectrics. [S0163-1829(98)05506-4]

I. INTRODUCTION

Ferroelectric properties reported recently for pyridinium tetrafluoroborate $[C_5H_6N]^+BF_4^-$,[1] denoted PyBF$_4$, were also found in other pyridinium salts.[2–4] A sequence of two phase transitions is characteristic of this family of ferroelectric crystals; PyBF$_4$ undergoes a ferroelectric-paraelectric phase transition at $T_1 = 238.7$ K, and another phase transition at $T_2 = 204$ K. Earlier second-moment NMR results[5–9] revealed a dynamical disorder of the ions in several pyridinium salts at room temperature, so the transformation at T_1 to the ferroelectric phase can be expected to be connected with ordering of the ions. In the present study, techniques of single-crystal x-ray and high-resolution powder neutron diffraction as well as dielectric measurements were employed for determining the structure of the PyBF$_4$ paraelectric phase, the symmetries of the low temperature phases, and directions and magnitudes of spontaneous polarization. They provide evidence for the multidimensional ferroelectric phase transition at T_1, and confirm that it is induced by ordering of the ions. The temperature dependences of the spontaneous polarization, electric permittivity, and crystal strain indicate clearly that the phase transition has a continuous character.

The transformation in the PyBF$_4$ crystals pertains to a long standing controversy concerning the character of phase transition in multidimensional ferroelectrics. Landau's theorems I and II relate the character of ferroelectric phase transitions to the orders of paraelectric and ferroelectric symmetry groups.[10] In these theorems a phase-transition index is defined as the ratio of the order of the paraelectric symmetry class divided by the order of the ferroelectric symmetry class.[11] According to the theorems, the phase transitions with index 2 may be continuous, and with index 3 are all of the first order. Meanwhile, the indices of phase transitions in hexagonal and cubic multidimensional ferroelectrics all are

equal or larger than 3. Coincidentally, no second-order phase transitions in multidimensional ferroelectrics were known. Although Landau's approach was later extended to higher values of the indices,[11–15] until recently[16] no single case of a continuous phase transition in a multidimensional ferroelectric was ever reported, to our knowledge. Therefore it was postulated, that in the multidimensional ferroelectrics a first-order character induced to the phase transition is due to the fluctuation of the order parameter.[17] Similarly, the reasons for the absence of experimental evidence of continuous transitions to incommensurate phases are currently investigated.[18] The transformation of PyBF$_4$ at T_1 fills the gap in the experimental evidence on the continuous phase transition in multidimensional ferroelectrics, and verifies Landau's method of deducting the character of phase transitions from symmetry considerations.

II. EXPERIMENTAL

Salt PyBF$_4$ is formed in the reaction between pyridine and tetrafluoroboric acid. Prior to our studies the substance obtained in this way was three times recrystallized. PyBF$_4$ crystals were grown from a water solution by slow evaporation at constant temperature. The maximum size of the grown rhombohedral crystals was $10 \times 10 \times 10$ mm. The habit of the crystals indicated that they belong to the trigonal system, similarly as the other pyridinium salts.[3,19,20] The PyBF$_4$ crystals are highly elastic and they are easily damaged by cutting. Even unshaped crystals often had broadened diffraction reflections. The x-ray structural studies were performed at 293 K on a single crystal of $0.2 \times 0.3 \times 0.2$ mm. A KUMA diffractometer with a graphite monochromator and ω-2Θ scan mode were applied. Two control reflections showed no significant intensity change throughout the data collection. The structure was solved[21] and refined by full-matrix least
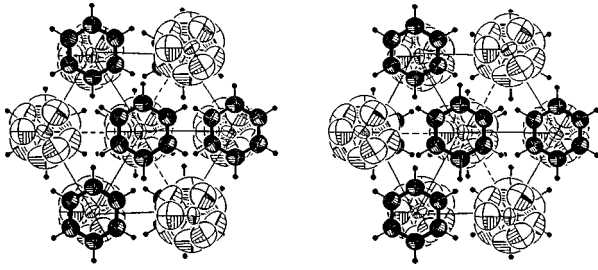
FIG. 1. An ORTEP stereoview of the $[C_5H_6N]^+BF_4^-$ rhombohedrical structure determined by x-ray at 296 K, down direction [111]. The thermal ellipsoids are drawn at 50% probability level, the H atoms are represented as small circles. The atoms of the $[C_5H_6N]^+$ cations are shaded for clarity. The sites of the disordered F atoms form nearly spherical distribution about well defined B atom at its center.

squares.[22] While the pyridine ring was located straightforwardly, the arrangement of peaks about the B atom approximated a regular octagon. After refining this initial model, new peaks appeared at about 1.4 Å from B, testifying to the orientational disorder of the BF_4 anions (see Fig. 1). The H site was located from a difference Fourier map. It was included in structure-factor calculations, but only its isotropic temperature factor was refined. The distribution of reflection intensities indicated a centrosymmetric space group. Nevertheless, the structure was refined in space groups $R\bar{3}m$ and $R3m$, however, the latter was rejected in the R-factor test.[23] The crystal data, as well as measurement and refinement details are summarized in Table I, the atomic parameters of the final model are listed in Table II.

Symmetry of the low-temperature phases was investigated by the powder method on deuterated $PyBF_4$ crystals using a high-resolution neutron powder diffraction at the Rutherford Appleton Laboratory.[24] A polycrystalline deuterated $PyBF_4$ was obtained as a product of the reaction between deuterated pyridine (99.5%) and fluoroboric acid. No isotope effect for T_1 and T_2 was confirmed by differential thermal analysis measurement. The compound was twice dissolved in heavy water and recrystallized. The powdered spectra were recorded at three temperatures: 293, 230, and 4.5 K. The powder data were analyzed by the program GSAS.[25]

Permittivity studies were performed at a frequency of 5 kHz using an impedance analyzer HP-4192A of Hewlett-Packard. Dielectric studies were carried out in the temperatures from 100 to 300 K for samples of the size $3 \times 3 \times 1$ mm in two directions: parallel and perpendicular to the threefold axis of the trigonal system. The hysteresis loop

TABLE I. Crystal data and details of the x-ray measurement of $PyBF_4$ at 293 K and of the structure refinement.

Formula	$[C_5H_6N]^+BF_4^-$
Molecular weight	166.9
Crystallographic system	trigonal
Space group	$R\bar{3}m$
a (Å)	5.673(1)
α (°)	97.33(1)
V (Å^3)	177.6(3)
Z	1
D_x (g/cm^3)	1.56
μ (Cu $K\alpha$) (mm^{-1})	1.49
$F(000)$ (e)	84
Reflections: collected	1853
observed ($I > 4\sigma_1$)	445
independent ($I > 4\sigma_1$)	108
R_{int}	0.031
R	0.12
wR	0.11
ΔF_{max} (e/Å^3)	0.14
ΔF_{min}	0.22
Max shift/σ	0.02

was recorded by a Diamant-Drenck-Pepinsky bridge on a digital oscilloscope Hewlett-Packard HP-5600B. Measurements of the pyroelectric effect were made by an electrometer type W-7-30.

III. RESULTS

A. Prototype phase structure

The unit cell comprises one pyridinium cation and one anion BF_4^-. Both ions are dynamically disordered. The pyridinium cation rotates around its axis perpendicular to the ring plane, but the positions of the so-disordered atoms N and C are well resolved in one symmetry-independent special position. Similarly, well resolved is the H atom. The cation is planar by symmetry requirements, the only independent dimensions are C-C* (each site contains 5/6 C and 1/6 N) of 1.3830(5) Å and C–H of 1.002 Å. The BF_4 anion is strongly disordered about the well-resolved B site. To model this disorder three symmetry-independent sites of the F atom have been included in the refinements; they are smeared with large temperature factors, as can be seen from the ORTEP (Ref. 26) drawing shown in Fig. 1. The angular dimensions of the anion cannot be reliably determined from this study,

TABLE II. Fractional atomic coordinates and thermal parameters (Å^2, isotropic for the H atom, and equivalent for the other atoms) for $PyBF_4$ in the paraelectric phase at 293 K.

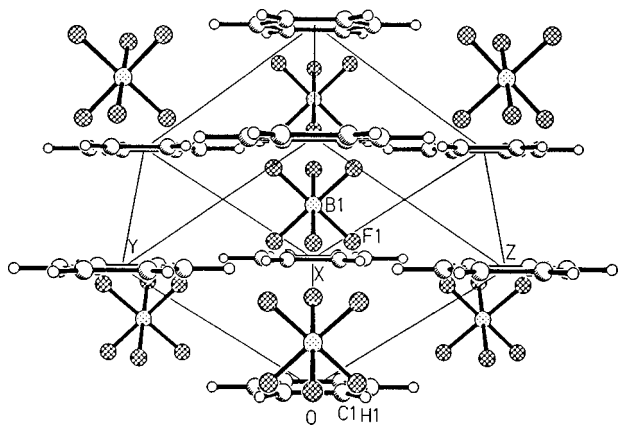| Atom	x/a	y/b	z/c	U_{eq}/U_{iso} (Å^2)
C(1)	0.1623(6)	$-0.1623(6)$	0	0.088(3)
H(1)	0.2800	-0.2800	0	0.17(4)
B(1)	0.5	0.5	0.5	0.089(5)
F(1)	0.2460(24)	0.4703(30)	0.4703(30)	0.159(9)
F(2)	0.5	$-0.3466(49)$	0.3466(49)	0.22(4)
F(3)	0.347(14)	0.347(14)	0.347(14)	0.12(6)

FIG. 2. Arrangement of the ions in $[C_5H_6N]^+BF_4^-$ viewed perpendicular to [111]: the same contents as in Fig. 1 is included. The ions are arranged alternatively along [111], for example in this drawing the bottom and top $[C_5H_6N]^+$ cations at 000 and 111 and the BF_4^- anion located at 1/21/21/2 in the center of the cell all lie on one of threefold axis. For clarity only six sites of disordered F atoms (these are symmetry related to F(1) in Table II and the text) have been shown in each of the anions.

but they can be found in literature.[27] The B-F(1), B-F(2), and B-F(3) distances are 1.415(13), 1.307(1), and 1.30(1) Å, respectively. The mean B-F distance of 1.365 Å in BF_4^- groups in the structures reported in literature[27] is also likely to be affected by disorder of the anions. The arrangement of the ions in the structure viewed perpendicular to the threefold axis is shown in Fig. 2.

B. Unit-cell transformation

The unit-cell dimensions measured at various temperatures are listed in Table III. The room-temperature results of the single-crystal x-ray and high-resolution neutron powder diffraction are in a very good agreement. The low-temperature neutron data confirm the transformation of the structure to the monoclinic C-type Bravais unit cell, as illustrated in Fig. 3. Apart from the dielectric measurements (see below) the transition to the monoclinic system is evident from the strain of the pseudorhombohedral unit cells from their prototypic dimensions, as listed in Table III and shown

in Fig. 4. Both distortions $(\alpha_r - \gamma_r)$ and c_r/a_r increase when the crystal is cooled below T_1. The systematic absences indicate that the crystal assumes the $C2$ symmetry. This agrees with the symmetry considerations for the possible type of the phase transitions.[28] The distortions do not change markedly below T_2 and the crystal remains monoclinic in the lowest temperature range. The systematic absences of Bravais lattice C disappear and the two-fold axis parallel to the **y** axis is contradicted only by the observation of a weak (050) reflection, as shown in Fig. 5.

C. Electric permittivity measurements

In the trigonal system the most characteristic directions are parallel and perpendicular to the threefold crystal axis. The direction along the threefold axis of the crystal is also its optic axis allowing precise adjustments of the samples by the technique of conoscopic figures. Figure 6 presents the temperature dependences of permittivity recorded on heating the sample cut out along the threefold axis, and for another sample cut out in the direction perpendicular to it. Two anomalies at T_2 and T_1 due to the phase transitions were observed. The critical behavior of permittivity recorded in the direction perpendicular to the threefold axis at T_1 reaches a value close to 6000 and testifies to the occurrence of a ferroelectric phase transition. Only a small anomaly observed at T_1 in the direction of threefold axis confirms that the ferroelectric properties are confined to the plane perpendicular to the threefold axis of the prototype phase. The anomaly at T_2 is considerably smaller and therefore indicates a nonferroelectric phase transition.

D. Ferroelectric hysteresis loop

The dielectric hysteresis loops recorded at 240.4, 237.4, and 235.2 K in the direction perpendicular to the threefold axis are shown in Fig. 7. The coercive field strongly rises with decreasing temperature, which allowed us to limit the temperature range of coercive field measurements to a few degrees below the Curie point. At 235 K, spontaneous polarization reaches a value of about 1 $\mu C/cm^2$, while the coercive field is of an order of 6 kV/cm. Observations of the hysteresis loops provided final confirmation of ferroelectric

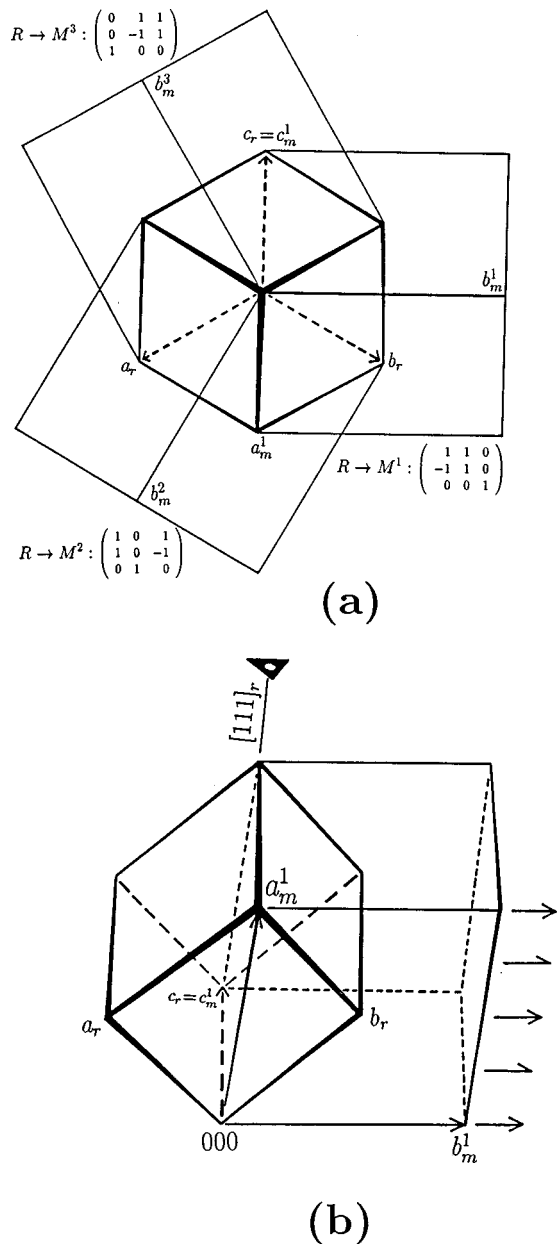TABLE III. Unit-cell dimensions (Å, °) of PyBF$_4$ measured at various temperatures. For 293 K the pseudomonoclinic and rhombohedral cell dimensions of prototypic structure are given, while for the temperatures below 238.7 K the dimensions of monoclinic Bravais C cell, and of the pseudorhombohedral cell are listed. The rhombohedral cell volume V_r is half of V_m. The estimated standard deviations in parentheses indicate the dimensions obtained from the Rietveld refinement on the powder data or from the least-squares fit to automatically centered single-crystal reflections; the pseudosymmetric cell dimensions are given without standard deviations. Subscripts m and r denote the monoclinic and rhombohedral reference systems, respectively.

T (K)	a_m	b_m	c_m	β_m	V_m	$a_r = b_r$	c_r	$\alpha_r = \beta_r$	γ_r
293	7.494	8.519	5.673	101.14	355.2	5.673(1)	$= a_r$	97.33(1)	$= \alpha_r$
293[a]	7.492	8.514	5.671	101.10	355.0	5.67074(7)	$= a_r$	97.305(1)	$= \alpha_r$
230[a]	7.3468(2)	8.3995(2)	5.7114(2)	101.952(2)	344.8	5.580	5.711	97.84	94.65
220[a]	7.317(3)	8.299(3)	5.7475(3)	102.250(2)	338.5	5.510	5.747	98.10	96.79
4.5[a]	7.2347(2)	8.1993(2)	5.6783(2)	103.403(2)	327.7	5.467	5.678	98.82	97.15

[a]High-resolution neutron powder-diffraction data.

$R \to M^3 : \begin{pmatrix} 0 & 1 & 1 \\ 0 & -1 & 1 \\ 1 & 0 & 0 \end{pmatrix}$

$R \to M^1 : \begin{pmatrix} 1 & 1 & 0 \\ -1 & 1 & 0 \\ 0 & 0 & 1 \end{pmatrix}$

$R \to M^2 : \begin{pmatrix} 1 & 0 & 1 \\ 1 & 0 & -1 \\ 0 & 1 & 0 \end{pmatrix}$

(a)

(b)

FIG. 3. Rhombohedrical cell of $[C_5H_6N]^+BF_4^-$ viewed down [111] and three monoclinic unit cells of six orientational states are shown in (a). The rhombohedrical versors are drawn with dashed arrows and denoted with subscript r. All versors of the monoclinic cell (subscript m) are indicated only for the orientational state 1 (superscript 1), while for the remaining two orientational states only the b_m axes are labeled. Also transformation matrices from the rhombohedrical cell to the monoclinical states are given. In (b) the rhombohedrical cell is viewed perpendicular to [111] and to the $\overline{3}$ axis, and only the first monoclinic orientational state with indicated 2 and 2_1 axes contained in the $a_m b_m$ plane is shown.

properties of PyBF$_4$ below T_1. High values of the coercive field hindered measurements of spontaneous polarization from the hysteresis loops in a wide temperature range, so we resorted to the studies of the pyroelectric effect. No detection of the hysteresis loop for the crystal cut out along the three-fold axis testifies to the location of the spontaneous polarization vectors in the (00.1) plane.
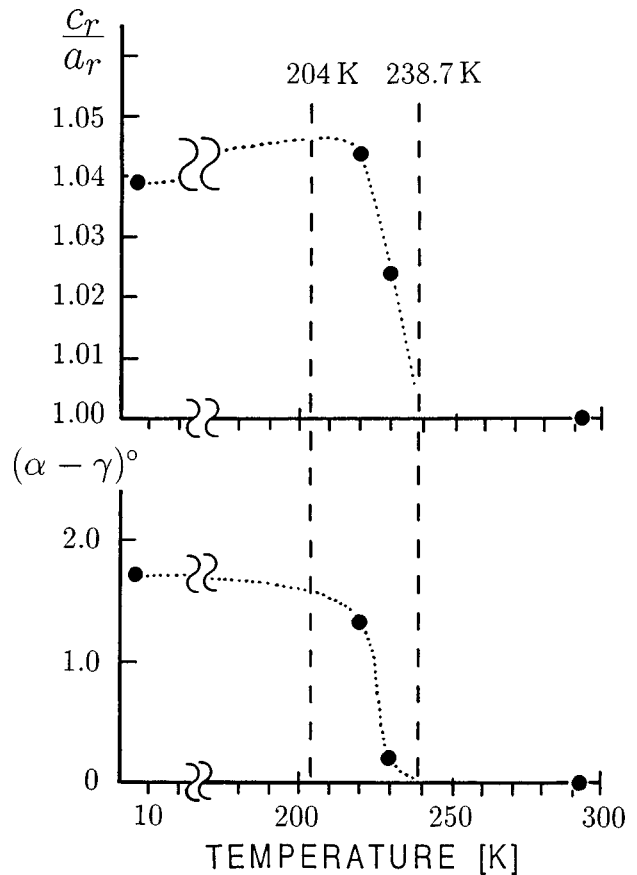

FIG. 4. Temperature dependence of the strain in the pseudo-rhombohedrical unit cell represented in term of the ratio c_r/a_r and of the difference between angles α and γ (see Table III). The dotted line has no physical meaning and is drawn merely for guiding the eyes. The estimated standard deviations are smaller than the size of the symbols (see the text).
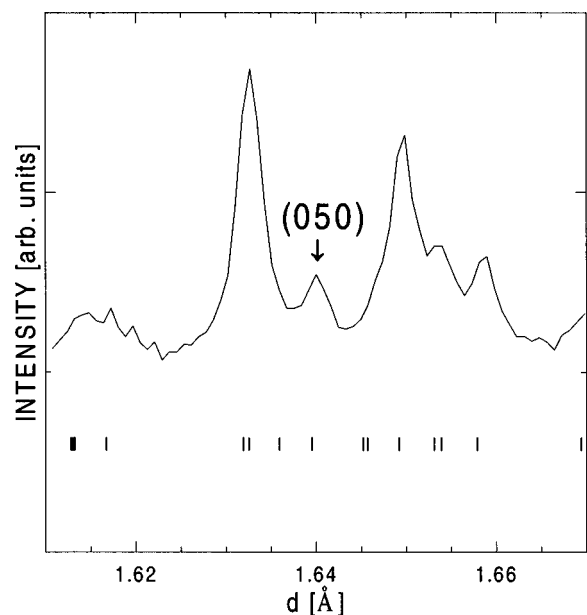

FIG. 5. Fragment of the high-resolution neutron powder-diffraction pattern recorded for $[C_5H_6N]^+BF_4^-$ with the indicated peak corresponding to reflection (050).
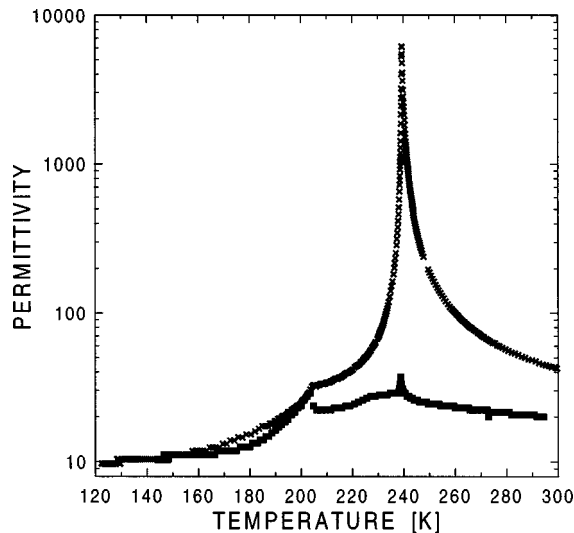
FIG. 6. Temperature dependence of electric permittivity measured in $[C_5H_6N]^+BF_4^-$ along (squares) and perpendicular (crosses) to the threefold axis.

E. Measurements of spontaneous polarization by the pyroelectric effect

The temperature changes of spontaneous polarization determined on the basis of pyroelectric-effect measurements are plotted in Fig. 8. The pyroelectric effect was measured in the range from 160 to 250 K. To pull the crystal into the single domain state, it was cooled at the rate 2 K/min in the electric field of an order of 4000 V/cm. The heating rate during the measurements was 0.5 K/min. The dependence of spontaneous polarization is nonzero, below T_2, and at 160 K it assumes the value of 1.5 $\mu C/cm^2$ which is characteristic of multidimensional ferroelectrics.[29] However, the nonferroelectric transition at T_2 is manifested as a small anomaly in the temperature dependence of spontaneous polarization. In temperatures above the T_1 Curie point spontaneous polarization vanishes, which additionally confirms that the symmetry of its prototype phase is centrosymmetric $R\bar{3}m$. The Curie-Weiss constant is another characteristic parameter of ferro-
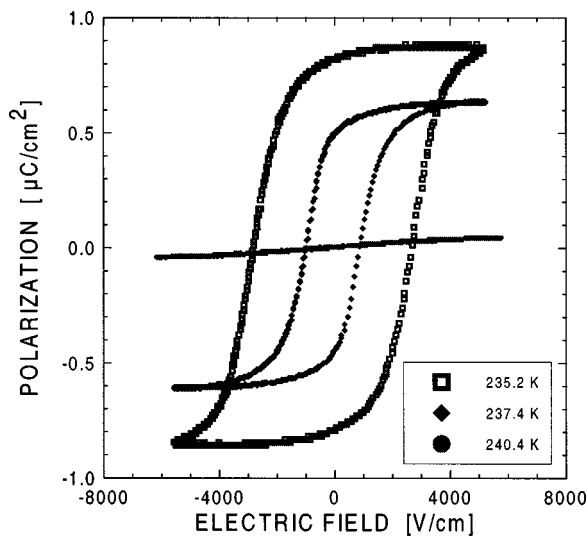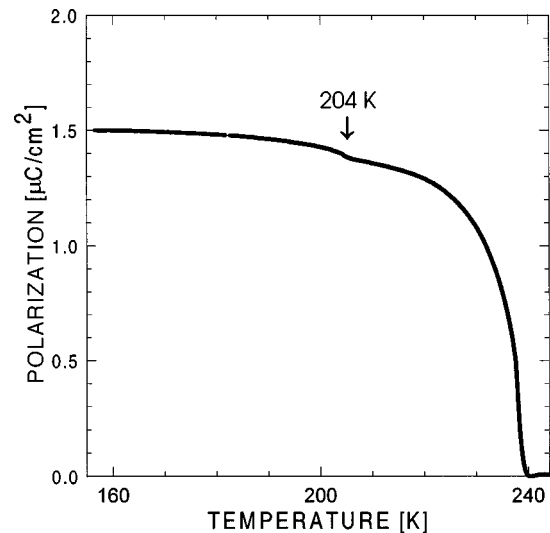
FIG. 8. Temperature dependence of spontaneous polarization in $[C_5H_6N]^+BF_4^-$ obtained from the pyroeffect measurements.

electrics. It equals 660 K, as determined from the linear dependence $1/\varepsilon(T)$ plotted in Fig. 9.

IV. DISCUSSION

The space group of the prototype phase of the PyBF$_4$ crystal in temperatures above the Curie point T_1, has been determined as $R\bar{3}m$ of the trigonal crystallographic system. Both cation and anion are located on a threefold inversion axis (see Figs. 1, 2, and 3). The disordered cations have additionally the symmetry of three mirror planes perpendicular to the bonds. Consequently, the disordered C and N atoms of the cation are distributed within one plane and exhibit a pseudohexagonal symmetry. The BF$_4$ group rotates in all directions and its shape resembles a sphere with the boron atom at its center. It is apparent that the symmetries of the cation or anion are inconsistent with the symmetries of their sites in space group $R\bar{3}m$, and that halting of any of the ionic
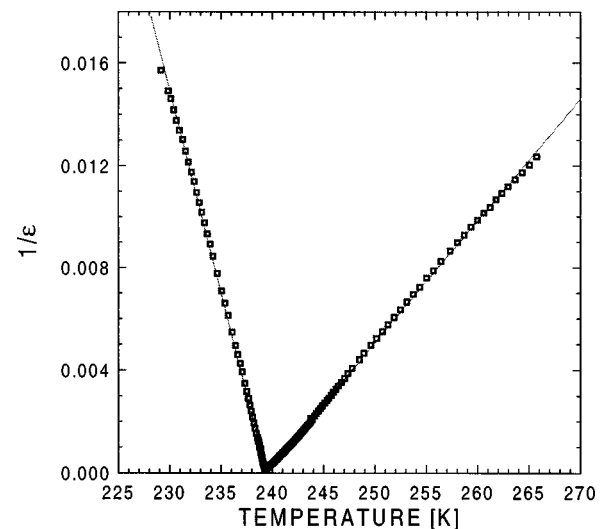
FIG. 7. Ferroelectric hysteresis loops recorded for $[C_5H_6N]^+BF_4^-$ at 240.4, 237.4, and 235.2 K.

FIG. 9. Temperature dependence of reciprocal electric permittivity closed to the ferroelectric phase transition at T_1 in $[C_5H_6N]^+BF_4^-$.

TABLE IV. Permissible symmetry relations between the prototypic $\bar{3}m$ point group and its ferroelectric subgroups.

Possible ferroelectric subgroups	Directions of polarization[a]	Number of spontaneous polarization directions
$3m$	$[111]$	2
2	$[10\bar{1}]$	6
m	$[h+l,l-h,1]$	6
1	$[hkl]$	12

[a]The equivalent directions referred to the hexagonal unit cell are $[00.1]$, $[11.0]$, $[h0.1]$, and $[h'k'.1']$.

rotations will result in breaking the crystal symmetry. According to Landau's theory, the number of symmetry elements is reduced at the phase transition.[28] All theoretically possible subgroups for ferroelectric phase transitions from the point group $\bar{3}m$ are compiled in Table IV. A transition to point group 1 of the triclinic system can be excluded on the grounds of the precise neutron-diffraction measurements of the lattice constants (Table III), which strongly indicate a transition to the monoclinic system. Another experimental verification of the crystal point symmetry is the direction of spontaneous polarization P_S. In the point group $3m$ the P_S vector would be directed along $[00.1]$ parallel to the threefold axis (Table IV), in the monoclinic symmetry class 2 P_S is perpendicular to the threefold axis of the prototype system, and in the monoclinic class m there are no restrictions for inclination between P_S and the threefold axis. The strong anisotropy of the permittivity (see Fig. 6) means that the ferroelectric direction is perpendicular to the threefold axis below T_1, and the crystal symmetry is described by the point group 2. The change of the crystallographic system is also indicated by splitting of $(hkk)_r$ diffraction reflections at 230 K (subscript r refers to the rhombohedral unit cell—see Table III). As further follows from the analysis of systematic absences among the reflections, the ferroelectric phase is described by the $C2$ space group of the monoclinic system. In the ferroelectric phase below T_1 spontaneous polarization assumes the directions of twofold axes retained of the prototype $R\bar{3}m$ space group. There are three coplanar twofold axes at every 60°, all perpendicular to the threefold axis of the prototype phase, as shown in Fig. 3. Thus, PyBF$_4$ is a multidimensional ferroelectric.

The continuous character of the phase transition at T_1 is confirmed both by the diffraction an dielectric measurements. The spontaneous strain in the ferroelectric phase recedes to zero when temperature rises to T_1, as shown in Fig. 4. The shape of the temperature dependence of permittivity is characteristic of the second-order phase transitions. To further verify this observation we analyzed the temperature dependence of the reverse permittivity, shown in Fig. 9. It is linear and does not reveal any discontinuities near the phase-transition point. The ratio of the slopes of $1/\varepsilon(T)$ in the ferroelectric and paraelectric phases is 3.3, which is only slightly higher than the value of 2, theoretically predicted for second-order phase transitions. This is usually considered convincing evidence of a second-order phase transition.[28] PyBF$_4$ is the an example of multidimensional ferroelectrics with the continuous phase transition. The index of the phase

transition at T_1 between $R\bar{3}m$ and $C2$ is equal to 6. According to Landau's Theorem I,[11] if the index of transformation equals 2, the thermodynamic potential is an even function of the order parameter and the phase transition *may be* continuous. According to Landau's Theorem II, if the index equals 3, the thermodynamic potential contains a cubic term with respect to order parameter and the phase transitions *are* of the first order. Theorem II applies to the structure of pyridinium perchlorate, denoted PyClO$_4$, undergoing at 247 K a clearly first-order[3] ferroelectric phase transition between space group $R3m$ and Cm (index of the transition equals 3). Although the postulated mechanism of the phase transition in PyClO$_4$ and PyBF$_4$ are both connected with the onset of ordering of the pyridinium cations, and their microstructures are similar, these phase transitions are different in character. It appears that this difference may be due to the symmetries, and consequently different indices of the transformations. While Landau's Theorems I and II apply only to transition indices 2 and 3, it was shown theoretically[11,12] that all possible phase transitions with an index equal to 6 may be continuous in character. All the cases with an index equal to 6 concern multidimensional transformations of trigonal, hexagonal or cubic prototype phases. The absence of experimental reports on any continuous phase transitions for multidimensional ferroic crystals suggested that such theoretically predicted phase transitions might not exist.[17] The phase transition in PyBF$_4$ at T_1 provides a unique example of a continuous phase transition in a multidimensional ferroelectric and supports the validity of Landau's approach predicting from symmetry considerations the behavior of crystals at their transitions.[30,31]

In the nonferroelectric phase transition at T_2, the possible symmetry changes according to the Landau's theory are from $C2$ to triclinic $P1$ or $P\bar{1}$, or monoclinic $P2$, $P2_1$, $P2/m$ or $P2_1/m$ space groups. Pyroelectric-effect measurements showed that below T_2 spontaneous polarization assumes a nonzero value, which means that the crystal cannot assume a symmetry of the centrosymmetric space groups, $P\bar{1}$, $P2/m$ or $P2_1/m$. According to the unit-cell dimensions determined by the neutron high-resolution powder diffraction, the crystal remains monoclinic below T_2. The two noncentrosymmetric space groups $P2$ and $P2_1$ can be discriminated by the systematic absences among diffraction reflections. For space group $P2_1$ reflections $(0k0)_m$ are systematically absent for odd k indices, while for space group $P2$ there are no systematic extinctions (subscript m indicates a monoclinic unit cell with its $[y]$ axis along the symmetry axis, as shown in Fig. 4). Figure 6 presents a fragment of a powder diffractogram in which reflection (050) is discernible. This single violation of the systematic absences does not exclude space group $P2_1$ of the crystal below T_2 as it may be due to the effect of multiple reflections in the sample. The differences between the $P2$ and $P2_1$ symmetries may result from minute changes in orientations of the ions which can be discriminated by the most precise high-resolution measurements only. This uncertainty requires further investigation. At this point, the postulated sequence of space group changes at the phase transitions in PyBF$_4$ is $R\bar{3}m$ to $C2$ at T_1, and to $P2$ or $P2_1$ at T_2.

V. CONCLUSIONS

A unique example of a continuous phase transition in the multidimensional ferroelectric of $PyBF_4$ has been characterized by diffraction and dielectric results. It corroborates Landau's approach in which the character of the phase transitions is deduced from the phase-transition indices.

The symmetry changes appear to be the main factor differentiating the character of phase transitions among the members of this family of multidimensional ferroelectric crystals. Thus, the phase transition in $PyBF_4$, $\bar{3}mF2$, is continuous, and in $PyClO_4$, $3mFm$, of the first order. Besides, the sequences of two phase transitions in these substances are similar, for example, in $PyClO_4$, $T_1 = 247$ K and T_2 $= 233$ K, in pyridinium perrhenate, denoted $PyReO_4$, T_1 $= 330$ K and $T_2 = 250$ K. The sequence of the phase transitions in $PyBF_4$ has been established as $R\bar{3}m$ to $C2$ at T_1 and $C2$ to $P2$ or $P2_1$ at T_2. The transformations are consistent with the observed disorder of the ions in the paraelectric phase above T_1. Further studies on the symmetries, structures, and phase transitions of these group of ferroelectrics are being carried out.

[1] P. Czarnecki, W. Nawrocik, Z. Pająk, and J. Wąsicki, Phys. Rev. B **49**, 1511 (1994).

[2] P. Czarnecki, W. Nawrocik, Z. Pająk, and J. Wąsicki, J. Phys. C **6**, 4955 (1994).

[3] P. Czarnecki, J. Wąsicki, Z. Pająk, R. Goc, H. Małuszyńska, and S. Habryło, J. Mol. Struct. **404**, 175 (1997).

[4] J. Wąsicki, P. Czarnecki, Z. Pająk, W. Nawrocik, and W. Szczepański, J. Chem. Phys. **107**, 576 (1997).

[5] J. Wąsicki, Z. Pająk, and A. Kozak, Z. Naturforsch. Teil A **45a**, 33 (1990).

[6] J. Wąsicki, W. Nawrocik, Z. Pająk, I. Natkaniec, and A. V. Belushkin, Phys. Status Solidi A **114**, 497 (1989).

[7] A. Kozak, J. Wąsicki, and Z. Pająk, Phase Transit. **57**, 153 (1996).

[8] J. Wąsicki, A. Kozak, Z. Pająk, P. Czarnecki, A. V. Belushkin, and M. A. Adams, J. Chem. Phys. **105**, 9470 (1996).

[9] J. Ripmeester, Can. J. Chem. **54**, 3453 (1976).

[10] L. D. Landau, Sov. Phys. JETP **7**, 19 (1937).

[11] N. Boccara, Ann. Phys. (N.Y.) **47**, 40 (1968).

[12] V. Janovec, Czech. J. Phys., Sect. B **25**, 1362 (1975).

[13] A. P. Levanyuk and D. G. Sannikov, Zh. Eksp. Teor. Fiz. **60**, 1109 (1971).

[14] Yu. M. Gufan, and V. P. Sachnenko, Zh. Eksp. Teor. Fiz. **63**, 1909 (1972).

[15] Yu. Gufan, Fiz. Tverd. Tela (Leningrad) **13**, 225 (1971).

[16] P. E. Tomaszewski, Phase Transit. **38**, 127 (1992).

[17] B. A. Strukov, and A. P. Levanyuk, *Fizicheskie osnovy segnetoelektricheskich yavleni v kristalach* (Nauka, Moskow, 1983), pp. 129–131.

[18] A. P. Levanyuk, J. Korean Phys. Soc. (to be published).

[19] H. von Hartl, Acta Crystallogr., Sect. B: Struct. Crystallogr. Cryst. Chem. **31**, 1781 (1975).

[20] R. F. Copeland, S. H. Conner, and E. A. Meyers, J. Phys. Chem. **70**, 1288 (1966).

[21] G. Sheldrick, SHELXS-86, Program for crystal structure determination, University of Göttingen, 1986.

[22] G. Sheldrick, SHELXL-93, Program for crystal structure determination, University of Göttingen, 1993.

[23] W. C. Hamilton, in *International Tables for X-Ray Crystallography. Vol. IV*, edited by J. A. Ibers and W. C. Hamilton (Kynoch, Birmingham, 1974), pp. 228–292.

[24] W. I. F. David, D. E. Akporiaye, R. M. Ibberson, and C. C. Wilson, Report RAL-88-103, Rutherford Appleton Laboratory, Chilton, England, 1988 (unpublished).

[25] R. B. von Dreele, and A. C. Larson, Report LAUR 86-748, Los Alamos National Laboratory, Los Alamos, 1990 (unpublished).

[26] C. K. Johnson, ORTEP, Report ORNL-3794, Oak Ridge National Laboratory, Tennessee, 1965 (unpublished).

[27] F. A. Allen, O. Kennard, D. G. Watson, L. Brammer, A. G. Orpen, and R. Taylor, J. Chem. Soc. Perkin Trans. II, S1 (1987).

[28] R. Blinc, and B. Zeks, *Soft modes in ferroelectrics and antiferroelectrics* (North-Holland, Amsterdam, 1974).

[29] S. C. Abrahams, and E. T. Keve, Ferroelectrics **2**, 129 (1971).

[30] L. D. Landau, *Collected Papers* (Pergamon, Oxford, 1965).

[31] J.-C. Toledano, and P. Toledano, *The Landau Theory of Phase Transitions* (World Scientific, Singapore, 1987).